Original Article

Relative apical sparing obtained with speckle tracking echocardiography is not a sensitive parameter for diagnosing light-chain cardiac amyloidosis

Pei-Na Huang^, Ya-Ni Liu, Xue-Qing Cheng, Hong-Yun Liu, Jun Zhang, Li Li, Jie Sun, Yi-Ping Gao, Rui-Rui Lu, Yi-Peng Gao, You-Bin Deng

Department of Medical Ultrasound, Tongji Hospital, Tongji Medical College, Huazhong University of Science and Technology, Wuhan, China

Contributions: (I) Conception and design: YB Deng, PN Huang; (II) Administrative support: YB Deng, YN Liu; (III) Provision of study materials or patients: PN Huang, YN Liu, HY Liu, J Zhang, L Li, J Sun; (IV) Collection and assembly of data: PN Huang, YP Gao, RR Lu, YP Gao; (V) Data analysis and interpretation: PN Huang, XQ Cheng; (VI) Manuscript writing: All authors; (VII) Final approval of manuscript: All authors.

Correspondence to: You-Bin Deng, MD, PhD. Department of Medical Ultrasound, Tongji Hospital, Tongji Medical College, Huazhong University of Science and Technology, 1095 Jiefang Road, Wuhan 430030, China. Email: ybdeng2007@hotmail.com.

Background: Distinguishing light-chain cardiac amyloidosis (AL CA) from left ventricular wall thickening (LVWT) resulted from other etiologies has proven to be challenging. This study aimed to determine the sensitivity and specificity of relative apical sparing in diagnosing AL CA and investigate the differences in clinical and echocardiographic characteristics between AL CA patients with apical sparing and those with non-apical sparing.

Methods: A total of 63 consecutive patients with AL CA, 102 consecutive patients with LVWT (including 51 hypertrophic cardiomyopathy (HCM) and 51 hypertension) and 33 healthy individuals were recruited retrospectively at Tongji Hospital, Tongji Medical College, Huazhong University of Science and Technology. Conventional and speckle tracking echocardiography were performed on all subjects.

Results: Although wall thickening was observed in all patients, almost all functional parameters were worse in AL CA, except for relative apical longitudinal strain (LS) (P=0.906). Of 63 patients with AL CA, only 17.5% (n=11) showed an apical sparing pattern. Patients with apical sparing had poorer cardiac performance than those with non-apical sparing. Relative apical sparing showed the lowest diagnostic accuracy with an area under the curve (AUC) of 0.58 [95% confidence interval (CI): 0.49–0.67, sensitivity: 17.5%, specificity: 98.0%, P=0.095] to detect AL CA, but right ventricular strain (RVS) (AUC: 0.86, P<0.001) showed the highest among all echocardiographic parameters. When diagnosing AL CA patients with non-apical sparing, RVS continued to maintain excellent diagnostic accuracy (AUC: 0.84, P<0.001), followed by left atrial reservoir strain (LASr) (AUC: 0.77, P<0.001).

Conclusions: The diagnostic value of relative apical sparing for AL CA was limited with low sensitivity. In clinical practice, the diagnosis of early AL CA patients should not solely rely on relative apical sparing.

Keywords: Light-chain cardiac amyloidosis (AL CA); speckle tracking echocardiography; relative apical sparing; left atrial strain (LAS); right ventricular strain (RVS)

Submitted Sep 10, 2023. Accepted for publication Jan 05, 2024. Published online Mar 07 2024.
doi: 10.21037/qims-23-1292
View this article at: https://dx.doi.org/10.21037/qims-23-1292

^ ORCID: 0000-0003-2902-464X.

© Quantitative Imaging in Medicine and Surgery. All rights reserved.

Introduction

Light-chain cardiac amyloidosis (AL CA) is a restrictive cardiomyopathy caused by deposition of amyloid fibrils derived from immunoglobulin light chains produced by clonal plasma cell disorders. Based on a real-world study, the incidence of light-chain amyloidosis is approximately 9.7–14.0 individuals per million person-years (1). Moreover, heart involvement is prevalent in over 50% of patients diagnosed with light-chain amyloidosis (2). The median survival time of patients with AL CA varies depending on the stage of cardiac involvement at diagnosis (3). Patients with advanced AL CA have a median survival of only 4 months, whereas patients with early-stage AL CA have a median survival of approximately 2 years (4). Two-dimensional echocardiography is considered as the first-line diagnostic imaging tool for AL CA, but it lacks specificity to precisely distinguish amyloid from non-amyloid infiltrative or hypertrophic heart diseases (5,6). Advances in speckle tracking echocardiography have enabled characterization of myocardial deformation, which may provide additional information to differentiate amyloid myocardial hypertrophy from that caused by hypertension (HT) or hypertrophic cardiomyopathy (HCM). Left ventricular relative apical sparing pattern of longitudinal strain (LS) identified through speckle tracking echocardiography is typically recognized as a sensitive and specific indicator of cardiac amyloidosis (CA) and is extensively utilized in clinical settings (7). Nevertheless, the diagnostic accuracy of relative apical LS has varied widely among different studies, ranging from 0.62 to 0.90 (8-12).

Recently, left atrial strain (LAS) and right ventricular strain (RVS) also have shown to be useful for identifying CA (13-15). Brand *et al.* (16) found that LAS had shown higher diagnostic accuracy in distinguishing CA from other etiologies of left ventricular wall thickening (LVWT) when compared to relative apical LS (CA =35, LVWT =19).

In this study, we aim to (I) determine the sensitivity and specificity of relative apical sparing in diagnosing AL CA among patients with different etiologies of LVWT (including AL CA, HCM and HT); (II) investigate the differences in clinical and echocardiographic characteristics between AL CA patients with apical sparing and those with non-apical sparing; (III) explore the diagnostic accuracy of conventional and speckle tracking echocardiography in differentiating AL CA from other etiologies of LVWT. We present this article in accordance with the STARD reporting checklist (available at https://qims.amegroups.com/article/view/10.21037/qims-23-1292/rc).

Methods

Study population

From September 2012 to September 2022, this retrospective study enrolled a total of consecutive 63 patients with AL CA, 51 patients with HCM, and 51 patients with HT at Tongji Hospital, Tongji Medical College, Huazhong University of Science and Technology. AL CA was determined in 63 patients by endomyocardial biopsy (n=2) or non-cardiac biopsy (n=61) with typical imaging findings (17). HCM was defined by an unexplained wall thickness ≥15 mm (without family history) or ≥13 mm (with family history) (18) and HT was confirmed if having a history of HT (defined as systolic blood pressure ≥130 mmHg or diastolic blood pressure ≥80 mmHg) and secondary wall thickening (defined as interventricular septum or left ventricular posterior wall ≥12 mm) on transthoracic echocardiography (19). Data on the clinical manifestations, laboratory tests, electrocardiography, and imaging findings, including echocardiography and cardiovascular magnetic resonance (CMR), were used for the diagnosis of HCM and secondary wall thickening caused by HT (5,20). Additionally, we recruited 33 age-matched healthy individuals from the communities to undergo echocardiography by posting recruitment advertisements. In all groups, shared exclusion criteria included individuals aged below 18, congenital heart defects, valvular heart disease and myocardial infarction. Basic demographic, clinical and laboratory data for all patients were collected from electronic medical records. The New York Heart Association (NYHA) stage was determined at admission and the laboratory results closest to the time of echocardiography were used (21). The study was conducted in accordance with the Declaration of Helsinki (as revised in 2013). The study was approved by the Medical Ethics Committee of Tongji Hospital, Tongji Medical College, Huazhong University of Science and Technology (No. TJ-IRB20220413) and informed consent was taken from all individual participants.

Echocardiography

Transthoracic echocardiography was performed on vivid E9 or E95 ultrasound machine (GE Medical System, Horten, Norway) equipped with a M5S transducer and all images were analyzed by EchoPAC version 204 (GE Vingmed, Horten, Norway). All performers responsible for image analysis were blinded to the information of participants.

© Quantitative Imaging in Medicine and Surgery. All rights reserved.

Table 1 Demographic and clinical characteristics of control and patient groups

Parameters	Control (n=33)	HCM (n=51)	HT (n=51)	AL CA (n=63)	P value
Age (years)	54±11	52±11	56±11	59±7 [‡]	<0.001
Male	13 (39.4)	34 (66.7) [†]	46 (90.2) [†‡]	42 (66.7) [†§]	<0.001
BMI (kg/m^2)	24.0±2.2	25.0±3.5	25.3±2.8	22.7±2.3 [†‡§]	<0.001
BSA (m^2)	1.70±0.16	1.77±0.18	1.83±0.15 [†]	1.70±0.14 [§]	<0.001
SBP (mmHg)	123 (113, 133)	136 (121, 150) [†]	160 (143, 171) [†‡]	113 (104, 129) [‡§]	<0.001
DBP (mmHg)	72 (68, 82)	85 (73, 97) [†]	89 (80, 98) [†]	72 (67, 77) [‡§]	<0.001
HR (bpm)	66 (60, 78)	74 (66, 83)	71 (64, 78)	78 (73, 87) [†§]	<0.001
NYHA III–IV stage	–	4/48 (8.3)	8/51 (15.7)	30/63 (47.6) [‡§]	<0.001
NT-proBNP (pg/mL)	–	803 (202, 1,806)	632 (54, 4,373)	3,564 (564, 8,769) [‡§]	<0.001
Troponin I (pg/mL)	–	20.8 (8.0, 47.5)	9.1 (4.6, 26.2)	59.9 (22.8, 150.9) [‡§]	<0.001
eGFR (mL/min)	–	83.1 (65.6, 100.9)	62.4 (14.8, 91.9) [‡]	69.5 (48.3, 89.0) [‡]	<0.001

Values are n (%), mean ± standard deviation, or median (interquartile range). [†], P<0.05, versus healthy control; [‡], P<0.05, versus patients with HCM; [§], P<0.05, versus patients with HT. HCM, hypertrophic cardiomyopathy; HT, hypertension; AL CA, light-chain cardiac amyloidosis; BMI, body mass index; BSA, body surface area; SBP, systolic blood pressure; DBP, diastolic blood pressure; HR, heart rate; NYHA, New York Heart Association; NT-proBNP, n-terminal pro-B-type natriuretic protein; eGFR, estimated glomerular filtration rate.

Analyses of ventricular and atrial strain

Apical 4-chamber, 2-chamber, and long-axis views were used to determine left ventricular global longitudinal strain (GLS) and regional LS (22) and the right ventricle focused 4-chamber apical view was used to determine RVS (23). The left ventricular relative apical LS was calculated according to the following formula:

$$relative\ apical\ \mathrm{LS} = \frac{average\ apical\ \mathrm{LS}}{average\ basal\ \mathrm{LS} + average\ mid\ \mathrm{LS}} \quad [1]$$

and the apical sparing pattern was defined as relative apical LS ≥1 (7).

Biplane left atrial LS curves were obtained from the optimized apical 4-chamber and 2-chamber views by tracing the left atrial endocardial border (23). To measure left atrial reservoir (LASr), conduit (LAScd), and contraction strain (LASct), left atrial LS was set to zero strain at the ventricular end-diastole in all subjects. Biplane LAS was the average of measurements obtained from apical 4-chamber and 2-chamber views.

Statistical analyses

SPSS 25.0 was utilized for statistical analyses in this study. For continuous variables, normally and non-normally distributed data were expressed as mean ± standard deviation and median and interquartile range, respectively. For categorical variables, data were expressed as number and percentage. Independent T test and one-way analysis of variance were used to compare normally distributed variables, Mann-Whitney U test and Kruskal-Wallis H test were used to compare non-normally distributed variables, and Chi-squared test and Fisher exact test were used to compare categorical variables. If there were significant differences among groups, a post hoc analysis was performed. To evaluate the diagnostic value of variables for AL CA, receiver operating characteristic curve (ROC) analyses were performed. All statistical tests were performed using a two-tailed approach. Statistical significance was determined by P value <0.05 or the corrected α level.

Results

Demographic and clinical characteristics

The detailed demographic and clinical characteristics of control and patient groups are shown in *Table 1*. Compared with AL CA group, the HCM group was younger and the HT group had a greater proportion of men. The percentage of patients with NYHA III–IV stage and levels of troponin I and n-terminal pro-B-type natriuretic protein

© Quantitative Imaging in Medicine and Surgery. All rights reserved.

Table 2 Comparisons of variables from echocardiography among groups

Parameters	Control (n=33)	HCM (n=51)	HT (n=51)	AL CA (n=63)	P value
IVS (mm)	9 (8, 10)	19 (18, 22)†	14 (13, 15)†‡	15 (13, 17)†‡	<0.001
LVPW (mm)	8 (8, 10)	11 (10, 13)†	13 (12, 14)†‡	14 (13, 16)†‡	<0.001
LVEF (%)	64 (61, 68)	59 (54, 64)†	60 (56, 64)†	53 (44, 59)†‡§	<0.001
LAVI (mL/m^2)	27.6±5.9	36.5±12.7†	30.5±8.1	35.6±10.9†	<0.001
RA area (cm^2)	13.8 (12.6, 15.4)	13.8 (12.3, 17.9)	14.6 (13.0, 17.2)	16.1 (13.4, 18.5)†	0.013
RV FWT (mm)	4 (4, 5)	5 (4, 6)	4 (4, 5)	6 (5, 7)†‡§	<0.001
RV FAC (%)	51.7±7.2	55.2±5.7	53.6±6.7	45.3±11.2†‡§	<0.001
TAPSE (mm)	23 (21, 24)	20 (18, 23)†	22 (19, 24)	13 (11, 18)†‡§	<0.001
E/A ratio	1.05 (0.85, 1.29)	0.78 (0.60, 1.13)†	0.81 (0.70, 1.01)†	0.95 (0.71, 1.29)	0.004
E/e' ratio	9.0 (7.5, 10.8)	12.4 (9.3, 15.8)†	10.6 (8.7, 13.1)	12.6 (9.9, 17.4)†§	<0.001
Mitral s' (cm/s)	9±1	7±2†	9±2‡	7±2†§	<0.001
Tricuspid s' (cm/s)	14±2	14±3	15±3	12±3†‡§	<0.001
PE	0 (0)	3 (5.9)	13(25.5)†‡	33 (52.4)†‡§	<0.001
GLS_{endo} (%)	−26.1±2.1	−18.1±4.8†	−21.3±3.0†‡	−15.1±5.3†‡§	<0.001
GLS_{mid} (%)	−22.4±1.8	−14.6±4.1†	−17.9±2.6†‡	−12.4±4.9†‡§	<0.001
GLS_{epi} (%)	−19.4±1.7	−11.9±3.6†	−15.0±2.4†‡	−10.4±4.6†§	<0.001
Relative apical LS	0.63 (0.61, 0.67)	0.74 (0.56, 0.84)†	0.72 (0.66, 0.79)†	0.69 (0.61, 0.84)†	0.002
Apical sparing pattern	0 (0)	2 (3.9)	0 (0)	11 (17.5)†‡§	<0.001
LASr (%)	36 (33, 41)	24 (21, 29)†	31 (25, 35)†‡	13 (9, 22)†‡§	<0.001
LAScd (%)	−20 (−16, −23)	−10 (−7, −14)†	−14 (−10, −17)†	−7 (−5, −11)†§	<0.001
LASct (%)	−16 (−14, −19)	−14 (−10, −17)	−17 (−13, −20)‡	−5 (-3, −13)†‡§	<0.001
RV GS (%)	−24.4±2.1	−23.1±4.0	−23.5±3.0	−16.9±4.9†‡§	<0.001
RV FWS (%)	−29.1±2.7	−29.5±5.1	−29.5±3.9	−21.4±5.9†‡§	<0.001

Values are n (%), mean ± standard deviation, or median (interquartile range).†, P<0.05, versus healthy control; ‡, P<0.05, versus patients with HCM; §, P<0.05, versus patients with HT. HCM, hypertrophic cardiomyopathy; HT, hypertension; AL CA, light-chain cardiac amyloidosis; IVS, interventricular septum; LVPW, left ventricular posterior wall; LVEF, left ventricular ejection fraction; LAVI, left atrial volume index; RA, right atrial; RV, right ventricular; FWT, free wall thickness; FAC, fractional area change; TAPSE, tricuspid annular systolic plane excursion; PE, pericardial effusion; GLS_{endo}, global longitudinal strain of subendocardial layer; GLS_{mid}, global longitudinal strain of mid layer; GLS_{epi}, global longitudinal strain of subepicardial layer; LS, longitudinal strain; LASr, left atrial reservoir strain; LAScd, left atrial conduit strain; LASct, left atrial contraction strain; GS, global strain; FWS, free wall strain.

(NT-proBNP) in AL CA group were significantly higher than those in HCM and HT (all P<0.001).

Conventional and speckle tracking echocardiography

Comparisons of echocardiographic variables among four groups are summarized in *Table 2*. Although left ventricular wall thickness thickened in all patient groups, functional measurements from conventional and speckle tracking echocardiography, including left ventricular ejection fraction, E/e' ratio, mitral average s' and GLS, were worse in AL CA. Of 63 patients with AL CA, only 17.5% showed an apical sparing pattern and there was no difference in relative apical LS among the three patient groups (P=0.906). Of note, apical sparing pattern was also observed in 3.9% (2/51) of patients with HCM.

© Quantitative Imaging in Medicine and Surgery. All rights reserved.

Table 3 Differences of clinical and echocardiographic characteristics between subgroups with non-apical sparing and apical sparing

Parameters	Non-apical sparing (n=52)	Apical sparing (n=11)	P value
Age (years)	59±8	58±7	0.67
Male	34 (65.4)	8 (72.7)	0.907
SBP (mmHg)	117 (101, 130)	110 (104, 110)	0.161
DBP (mmHg)	72 (67, 76)	74 (70, 78)	0.698
NYHA III–IV stage	21 (40.4)	10 (90.9)	<0.001
NT-proBNP (pg/mL)	3,240 (545, 7,172)	4,780 (3,067, 25,431)	0.096
Troponin I (pg/mL)	59.0 (18.9, 121.0)	67.0 (29.9, 634.0)	0.197
IVS (mm)	15±2	16±3	0.202
LVPW (mm)	14±2	16±3	0.001
LVEF (%)	53±9	42±10	0.001
E/A ratio	0.90 (0.67, 1.26)	1.16 (0.94, 2.07)	0.03
E/e' ratio	12.4 (9.7, 16.5)	16.8 (10.8, 24.2)	0.065
Mitral s' (cm/s)	7±2	6±2	0.061
Tricuspid s' (cm/s)	12±3	10±3	0.027
GLS_{endo} (%)	−15.2 (−12.2, −20.6)	−9.0 (−8.0, −17.0)	0.005
GLS_{mid} (%)	−11.7 (−9.4, −17.7)	−7.0 (−6.2, −14.3)	0.009
GLS_{epi} (%)	−10.7 (−7.8, −14.8)	−5.0 (−4.2, −12.2)	0.007
LASr (%)	17 (11, 23)	8 (6, 10)	0.001
LAScd (%)	−8 (−5, −11)	−6 (−4, −7)	0.028
LASct (%)	−8 (−4, −15)	−2 (0, −3)	<0.001
RV GS (%)	−17.6±4.7	−13.4±4.2	0.012
RV FWS (%)	−22.1±5.8	−17.9±5.0	0.035

Values are n (%), mean ± standard deviation, or median (interquartile range). Apical sparing pattern is defined as relative apical LS ≥1. SBP, systolic blood pressure; DBP, diastolic blood pressure; NYHA, New York Heart Association; NT-proBNP, n-terminal pro-B-type natriuretic protein; IVS, interventricular septum; LVPW, left ventricular posterior wall; LVEF, left ventricular ejection fraction; GLS_{endo}, global longitudinal strain of subendocardial layer; GLS_{mid}, global longitudinal strain of mid layer; GLS_{epi}, global longitudinal strain of subepicardial layer; LASr, left atrial reservoir strain; LAScd, left atrial conduit strain; LASct, left atrial contraction strain; RV, right ventricular; GS, global strain; FWS, free wall strain.

Although there was no statistically significant difference in left atrial volume index among the three patient groups, all three phasic LAS were markedly reduced in AL CA compared to HCM or HT. Similarly, the right atrial area was larger and right ventricular (RV) systolic function was poorer in AL CA, including smaller RV fractional area change, much more decreased tricuspid annular systolic plane excursion (TAPSE) and tricuspid s' wave, and worse deformation.

Patients with AL CA were divided into two subgroups based on the presence or absence of apical sparing pattern and *Table 3* illustrates the differences in clinical and echocardiographic characteristics between subgroups. In comparison to patients without apical sparing, individuals with apical sparing exhibited a greater prevalence of NYHA III–IV stage, along with elevated levels of troponin I and NT-proBNP. As for echocardiographic assessment, patients with apical sparing showed not only significantly poorer left ventricular function, but also markedly worse LAS and RVS (*Figures 1*,*2*).

© Quantitative Imaging in Medicine and Surgery. All rights reserved.

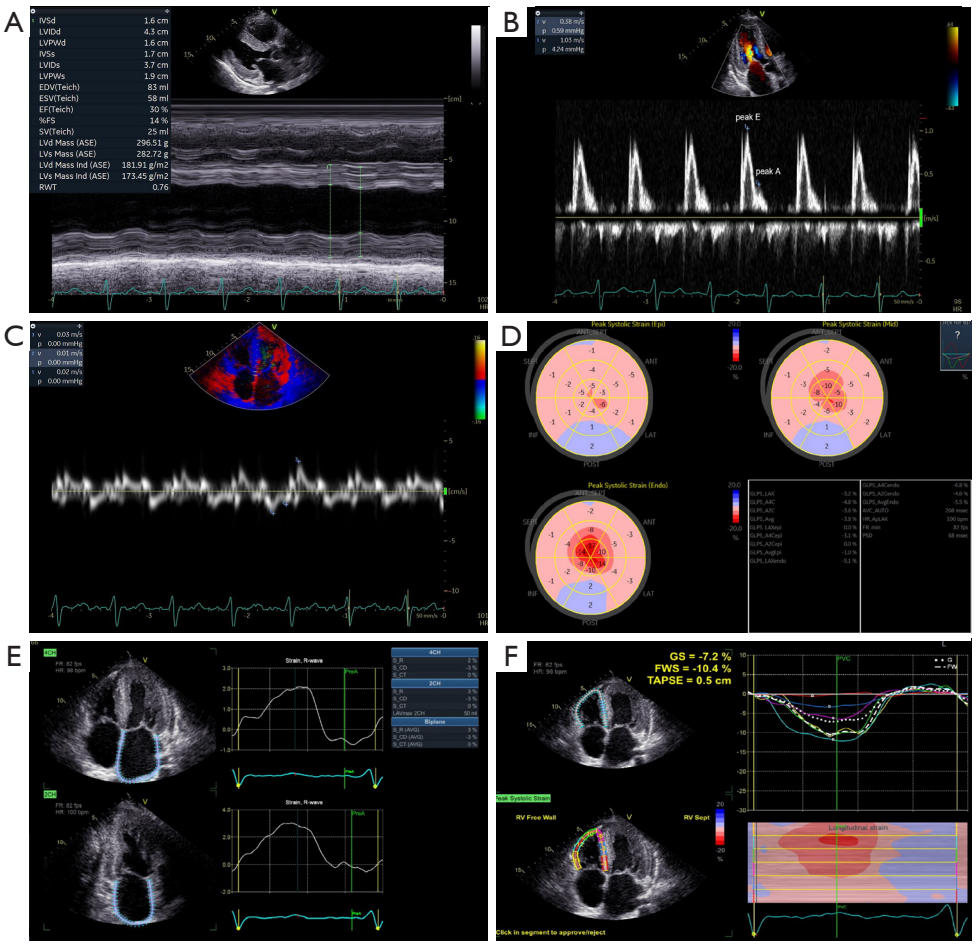

Figure 1 Conventional and speckle tracking echocardiography in a 50-year-old male patient with light-chain cardiac amyloidosis and apical sparing. New York Heart Association stage was IV, serum NT-proBNP was 5,770 pg/mL, and serum troponin I was 29.9 pg/mL. M-mode echocardiogram exhibited increased left ventricular wall and decreased left ventricular ejection fraction of 30% (A). Peak E wave velocity was 103 cm/s, peak A wave velocity was 38 cm/s, and E/A ratio was 2.71 on mitral inflow pulsed-wave Doppler recording (B). Septal mitral annular velocities e', a' and s were 2, 1 and 3 cm/s, respectively, and E/e' ratio was 51.5 on tissue Doppler recording (C). (D) was a bull's eye plot of left ventricular longitudinal strain. Global longitudinal strain was –3.8% and relative apical longitudinal strain was 1.72. (E) showed the results of biplane left atrial strain analysis, with left atrial reservoir strain of 3%, left atrial conduit strain of –3% and left atrial contraction strain of 0. (F) showed the results of right ventricular strain analysis. Right ventricular global strain, free wall strain and tricuspid annular systolic plane excursion were –7.2%, –10.4% and 5 mm, respectively. IVSd, diastolic interventricular septum; LVIDd, diastolic left ventricular internal diameter; LVPWd, diastolic left ventricular posterior wall; IVSs, systolic interventricular septum; LVIDs, systolic left ventricular internal diameter; LVPWs, systolic left ventricular posterior wall; EDV(Teich), end-diastolic volume; ESV(Teich), end-systolic volume; EF(Teich), ejection fraction; FS, fractional shortening; SV(Teich), stroke volume; LVd Mass (ASE), diastolic left ventricular mass; LVs Mass (ASE), systolic left ventricular mass; LVd Mass Ind (ASE), diastolic left ventricular mass index; LVs Mass Ind (ASE), systolic left ventricular mass index; RWT, relative wall thickness; HR, heart rate; peak E, peak early diastolic mitral inflow velocity; peak A, peak late diastolic mitral inflow velocity; v, velocity; p, pressure gradient; epi, subepicardial layer; mid, mid layer; endo, subendocardial layer; SEPT, septum; ANT_SEPT, anteroseptum; ANT, anterior wall; LAT, lateral wall; POST, posterior wall; INF, inferior wall; GLPS_LAX, global longitudinal peak strain of apical long-axis view; GLPS_A4C, global longitudinal peak strain of apical four-chamber view; GLPS_A2C, global longitudinal peak strain of apical two-chamber; GLPS_Avg, average global longitudinal peak strain; AVC_AUTO, auto aortic valve closing time; HR_ApLAX, heart rate from apical long-axis view; bpm, beats per minute; FR min, minimal frame rate; fps, frames per second; PSD, peak strain dispersion; FR, frame rate; 4CH, four-chamber view; 2CH, two-chamber view; AVG, average; S_R, reservoir strain; S_CD, conduit strain; S_CT, contraction strain; LAVmax 2CH, maximum left atrial volume of two-chamber view; preA, defined as onset of the A-wave in the mitral inflow profile; GS, global strain; FWS, free wall strain; TAPSE, tricuspid annular systolic plane excursion; PVC, pulmonary valve closing time; G, global strain; FW, free wall strain; RV, right ventricular.

© Quantitative Imaging in Medicine and Surgery. All rights reserved.

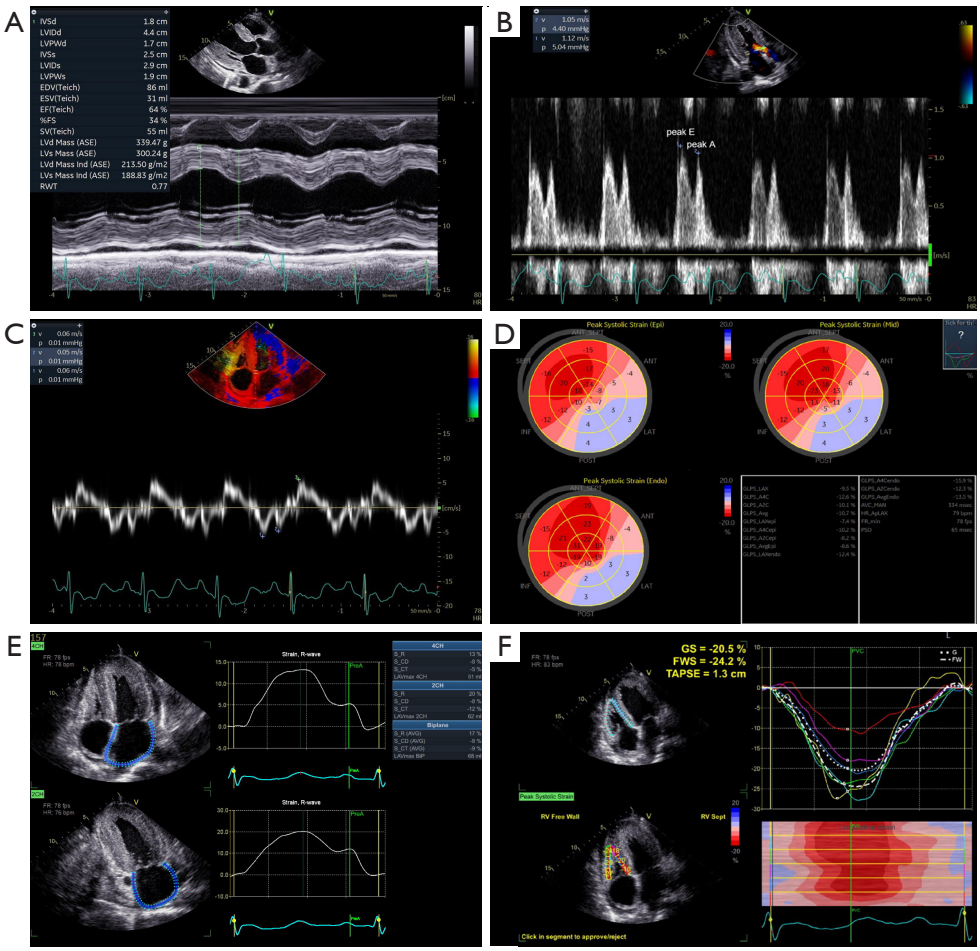

Figure 2 Conventional and speckle tracking echocardiography in a 53-year-old male patient with light-chain cardiac amyloidosis and non-apical sparing. New York Heart Association stage was III, serum NT-proBNP was 1,519 pg/mL, and serum troponin I was 4.7 pg/mL. M-mode echocardiogram exhibited increased left ventricular wall and preserved left ventricular ejection fraction of 64% (A). Peak E wave velocity was 112 cm/s, peak A wave velocity was 105 cm/s, and E/A ratio was 1.07 on mitral inflow pulsed-wave Doppler recording (B). Septal mitral annular velocities e', a' and s were 6, 5 and 6 cm/s, respectively, and E/e' ratio was 18.7 on tissue Doppler recording (C). (D) was a bull's eye plot of left ventricular longitudinal strain. Global longitudinal strain was –10.7% and relative apical longitudinal strain was 0.87. (E) showed the results of biplane left atrial strain analysis, with left atrial reservoir strain of 17%, left atrial conduit strain of –8% and left atrial contraction strain of –9%. (F) showed the results of right ventricular strain analysis. Right ventricular global strain, free wall strain and tricuspid annular systolic plane excursion were –20.5%, –24.2% and 13 mm, respectively. IVSd, diastolic interventricular septum; LVIDd, diastolic left ventricular internal diameter; LVPWd, diastolic left ventricular posterior wall; IVSs, systolic interventricular septum; LVIDs, systolic left ventricular internal diameter; LVPWs, systolic left ventricular posterior wall; EDV(Teich), end-diastolic volume; ESV(Teich), end-systolic volume; EF(Teich), ejection fraction; FS, fractional shortening; SV(Teich), stroke volume; LVd Mass (ASE), diastolic left ventricular mass; LVs Mass (ASE), systolic left ventricular mass; LVd Mass Ind (ASE), diastolic left ventricular mass index; LVs Mass Ind (ASE), systolic left ventricular mass index; RWT, relative wall thickness; HR, heart rate; peak E, peak early diastolic mitral inflow velocity; peak A, peak late diastolic mitral inflow velocity; v, velocity; p, pressure gradient; epi, subepicardial layer; mid, mid layer; endo, subendocardial layer; SEPT, septum; ANT_SEPT, anteroseptum; ANT, anterior wall; LAT, lateral wall; POST, posterior wall; INF, inferior wall; GLPS_LAX, global longitudinal peak strain of apical long-axis view; GLPS_A4C, global longitudinal peak strain of apical four-chamber view; GLPS_A2C, global longitudinal peak strain of apical two-chamber; GLPS_Avg, average global longitudinal peak strain; AVC_AUTO, auto aortic valve closing time; HR_ApLAX, heart rate from apical long-axis view; bpm, beats per minute; FR min, minimal frame rate; fps, frames per second; PSD, peak strain dispersion; FR, frame rate; 4CH, four-chamber view; 2CH, two-chamber view; AVG, average; S_R, reservoir strain; S_CD, conduit strain; S_CT, contraction strain; LAVmax 2CH, maximum left atrial volume of two-chamber view; preA, defined as onset of the A-wave in the mitral inflow profile; GS, global strain; FWS, free wall strain; TAPSE, tricuspid annular systolic plane excursion; PVC, pulmonary valve closing time; G, global strain; FW, free wall strain; RV, right ventricular.

© Quantitative Imaging in Medicine and Surgery. All rights reserved.

Table 4 ROC analyses of main echocardiographic parameters to detect light-chain cardiac amyloidosis among patients with left ventricular wall thickening

Parameters	AUC	95% CI	Cut-off	Sensitivity (%)	Specificity (%)	P value
E/e' ratio	0.60	0.52–0.69	11.0	66.7	50.0	0.026
GLS_{mid} (%)	0.73	0.64–0.81	–12.6	58.7	85.3	<0.001
Relative apical sparing	0.58	0.49–0.67	1.0	17.5	98.0	0.095
LASr (%)	0.80	0.73–0.88	23	82.5	69.6	<0.001
LAScd (%)	0.71	0.63–0.80	–9	57.1	77.5	<0.001
LASct (%)	0.79	0.71–0.87	–10	65.1	87.3	<0.001
RV GS (%)	0.86	0.80–0.92	–21.0	81.0	81.4	<0.001
RV FWS (%)	0.86	0.80–0.92	–26.4	79.4	81.4	<0.001

ROC, receiver operating characteristic curve; AUC, area under the curve; 95% CI, 95% confidence interval; GLS_{mid}, global longitudinal strain of mid layer; LASr, left atrial reservoir strain; LAScd, left atrial conduit strain; LASct, left atrial contraction strain; RV, right ventricular; GS, global strain; FWS, free wall strain.

Table 5 ROC analyses of main echocardiographic parameters to detect light-chain cardiac amyloidosis with non-apical sparing among patients with left ventricular wall thickening

Parameters	AUC	95% CI	Cut-off	Sensitivity (%)	Specificity (%)	P value
E/e' ratio	0.57	0.48–0.67	10.9	65.4	50.0	0.14
GLS_{mid} (%)	0.69	0.60–0.79	–12.6	55.8	85.3	<0.001
LASr (%)	0.77	0.69–0.83	23	78.8	69.6	<0.001
LAScd (%)	0.68	0.60–0.76	–10	63.5	67.6	<0.001
LASct (%)	0.75	0.67–0.81	–13	71.2	75.5	<0.001
RV GS (%)	0.84	0.77–0.89	–21.0	76.9	81.4	<0.001
RV FWS (%)	0.84	0.77–0.89	–26.4	75.0	81.4	<0.001

ROC analyses excluded AL CA patients with apical sparing. ROC, receiver operating characteristic curve; AUC, area under the curve; 95% CI, 95% confidence interval; GLS_{mid}, global longitudinal strain of mid layer; LASr, left atrial reservoir strain; LAScd, left atrial conduit strain; LASct, left atrial contraction strain; RV, right ventricular; GS, global strain; FWS, free wall strain; AL CA, light-chain cardiac amyloidosis.

Diagnostic value of echocardiographic parameters

Table 4 shows the diagnostic value of echocardiographic parameters in differentiating AL CA from other etiologies of LVWT. Relative apical sparing had the lowest diagnostic value among all echocardiographic parameters, but RVS had the highest. It was worth noting that among all echocardiographic parameters, the diagnostic specificity of relative apical sparing was the highest, while its sensitivity was the lowest. Additionally, the diagnostic value of LASr was highest among three phasic LAS.

In 52 AL CA patients with non-apical sparing, the diagnostic accuracy of echocardiographic parameters is shown in *Table 5*. Although there was a slight decline in the area under the curve (AUC) for all echocardiographic parameters when diagnosing AL CA patients with non-apical sparing, RVS continued to maintain excellent diagnostic accuracy, followed by LASr.

Discussion

Our study demonstrated that relative apical sparing had the highest specificity and the lowest sensitivity for diagnosing AL CA among all echocardiographic parameters in our study. Moreover, it was more frequently observed in advanced stage of AL CA, suggesting that patients with apical sparing were often in a deteriorated clinical condition

© Quantitative Imaging in Medicine and Surgery. All rights reserved.

accompanied by worse echocardiographic characteristics than those with non-apical sparing. In clinical practice, the integration of other sensitive parameters, particularly LAS and RVS, facilitated the early detection of patients with AL CA who were devoid of the characteristic apical sparing pattern.

Relative apical sparing

Although previous studies (7,9,11) have proven that apical sparing of LS is sensitive and specific to CA, our study revealed its limited diagnostic accuracy with high specificity and low sensitivity. Notably, diagnostic accuracy of apical sparing pattern was obtained by comparing CA patients with different subjects in previous studies (7,9,11). Phelan *et al.* (7) conducted a study to distinguish patients with CA from patients with either HCM or aortic stenosis (cut-off value: relative apical LS ≥1.0, AUC: 0.94, sensitivity: 93%, specificity: 82%). The study conducted by Nicol *et al.* (9) included patients with amyloidosis with or without cardiac involvement (cut-off value: relative apical LS≥0.90, AUC: 0.90, sensitivity: 73%, specificity: 96%). Additionally, Boldrini *et al.* (11) conducted a multi-center study with the objective of diagnosing cardiac involvement in patients with systemic light-chain amyloidosis (cut-off value: relative apical LS >1.0, AUC: 0.75, sensitivity: 58%, specificity: 83%) and identifying CA in patients with ventricular wall thickening (cut-off value: relative apical LS >0.9, AUC: 0.77, sensitivity: 71%, specificity: 73%). However, only 17.5% of patients with AL CA showed apical sparing pattern in our study. Similar to our results, there was no statistically significant difference in relative apical LS between CA and HCM groups in a CMR study and the AUC of relative apical LS was only 0.66 when relative apical LS >1.05 was used to differentiate patients with CA from those with either HCM or Anderson-Fabry's disease (10). Additionally, only 24 patients with CA (50%) had relative apical sparing according to Löfbacka *et al.* (24) We acknowledge that increasing the cut-off value decreases the diagnostic sensitivity of relative apical LS. However, the apical sparing pattern, defined as relative apical LS ≥1.0, remains the most commonly used and convenient cut-off value in clinical practice (5). Based on the presence or absence of apical sparing pattern, our subgroup analysis found that patients with apical sparing exhibited worse cardiac performance, including worse NYHA stage, worse left ventricular circumferential and longitudinal systolic function, worse three phasic LAS and worse RV longitudinal systolic function. Moreover, GLS reduction at all myocardial sublayers were more significant in patients with apical sparing than patients with non-apical sparing. Interestingly, Huntjens *et al.* (25) also found that the relative apical LS was significantly lower in patients with high LASr or high GLS than in patients with low LASr or low GLS (0.86 *vs.* 1.00, P<0.001). Hence, we have grounds to believe that left ventricular apical sparing pattern is closely associated with the progression of AL CA, which manifests in the later stage of the disease. Ternacle *et al.* (26) certified that reduced apical LS indicated severe amyloid deposition and tissue remodeling by combining histological and imaging findings, which implies that basal-to-apical gradient would disappear when there was extensive amyloid deposition in the apical section like the basal. However, Licordari *et al.* (27) discovered that among patients with early mutant transthyretin-related CA, the mid-basal LS emerged as the independent prognostic indicator, while the presence of apical sparing of LS did not predict cardiac death.

The considerable variability in diagnostic value of relative apical sparing among different studies can be attributed to the different stages of disease progression in the recruited subjects with AL CA. In the study by Phelan *et al.* (7), CA patients exhibited worse diastolic and systolic function than those in our study (E/A ratio: 2.2 *vs.* 0.95; E/e' ratio: 24.1 *vs.* 12.6; ejection fraction: 47% *vs.* 53%; GLS: –8.9% *vs.* –12.4%), while Boldrini *et al.* (11) reported higher level of NT-proBNP in CA group than that in our study. The research conducted by Williams *et al.* (10) included patients with CA at an earlier stage of the disease (GLS: –15.7%±4.6%) and unveiled that the AUC of relative apical sparing in distinguishing patients with CA from HCM and Anderson-Fabry's disease was only 0.66 [95% confidence interval (CI): 0.55–0.76], with a sensitivity of 43.0% and specificity of 82.0%.

Left atrial and RV function

AL CA is an infiltrative cardiomyopathy in which amyloid can deposit into all of chambers of the heart. While there was no difference in left atrial volume index between AL CA and LVWT groups, phasic LAS in AL CA was significantly lower compared to patients with LVWT caused by other etiologies. In recent years, LAS has been recognized as a reliable and sensitive tool for assessing left atrial function, thus becoming increasingly valued in the diagnostic workflow for CA. On the one hand, left ventricular systolic and diastolic dysfunction caused by amyloid deposition can

© Quantitative Imaging in Medicine and Surgery. All rights reserved.

result in secondary left atrial dysfunction (28). On the other hand, the left atrial amyloid deposition may lead to wall thickening and reduced compliance, which directly affects left atrial function. Even in discerning AL CA patients with non-apical sparing, LAS demonstrated a remarkable diagnostic accuracy in our study. Similar findings have also been observed by Sciacca and colleagues in a CMR research (29). Aimo *et al.* (15) found that LAS was the most valuable parameter for diagnosing AL CA through multi-chamber speckle tracking imaging.

Amyloid deposits were also found in the RV. Bodez *et al.* (30) found that RV late gadolinium enhancement was present in 62% of patients with CA, indicating amyloid deposition and myocardial fibrosis in the RV. Moñivas *et al.* (31) demonstrated that RV free wall strain in CA was significantly lower than that of healthy subjects and Licordari *et al.* (32) found that RVS was reduced in the early stage of familial transthyretin-related CA. In our study, both conventional (such as TAPSE and tricuspid s' wave) and speckle tracking echocardiography (such as RVS) showed severe RV dysfunction in AL CA. Furthermore, Di Bella *et al.* (33) conducted a study that identified additional echocardiographic findings beyond the left ventricle, such as the anterior ascending aortic wall and Eustachian valve, to possess good diagnostic value for CA. Shi *et al.* (34) found that left ventricular myocardial work index was associated with short-term prognosis in patients with AL CA. These studies collectively suggest that CA should be regarded as a whole-heart infiltrative cardiomyopathy. Therefore, in addition to apical sparing pattern, it is crucial to take into account other parameters, particularly LAS and RVS, to improve the detection rate of AL CA in echocardiography.

Limitations

Several limitations should be noted. Firstly, this study was a small-sample, single-center study. The diagnostic value of LAS and RVS for AL CA patients with non-apical sparing needs to be further validated in diverse healthcare facilities. Secondly, the lack of information regarding patient follow-up hampers the comprehensive understanding of long-term dynamics associated with the studied conditions. Follow-up study should be performed to determine the prognostic values of various echocardiographic parameters in the future. Thirdly, the diagnosis of HCM in our study population was not confirmed through pathological evidence. Consequently, the incomplete exclusion of CA in patients with HCM may affect the strength and reliability of our results. Nevertheless, a meta-analysis conducted by Aimo *et al.* (35) revealed that the prevalence of CA in patients with HCM was approximately only 7%, indicating that its impact on our results would not be significant. Similarly, myocardial biopsy was not performed in all patients with HT. It is possible that amyloidosis may be present in patients with HT in our study. However, the diagnosis of myocardial hypertrophy caused by HT was based on the clinical manifestations, laboratory tests, electrocardiography, and echocardiographic features, which are different from those of CA. Therefore, we believe that the incomplete exclusion of CA in patients with HT would not significantly impact the results of this study. Finally, in individuals with AL CA, amyloid deposition occurs in all cardiac chambers, resulting in thickening of the RV wall as well. However, this study focused solely on patients with LVWT. Furthermore, it should be noted that since this study was conducted retrospectively, there is a possibility of bias due to errors in records or missing data in a small subset of patients. However, it is worth mentioning that the percentage of missing data in our study was less than 10%, and its impact on the accuracy of estimates may not be significant.

Conclusions

To sum up, our study demonstrated that the diagnostic value of relative apical sparing for AL CA was limited, with the highest specificity and the lowest sensitivity among all echocardiographic parameters. Apical sparing pattern was typically observed in the later stage of AL CA. In clinical practice, the integration of other sensitive parameters, particularly LAS and RVS, is crucial for enhancing the early detection rate of AL CA.

Acknowledgments

The authors would like to thank the patients and their families for their participation and clinical staffs from the Department of Hematopathology and Medical Ultrasound for their supports.
Funding: None.

Footnote

Reporting Checklist: The authors have completed the STARD reporting checklist. Available at https://qims.amegroups.com/article/view/10.21037/qims-23-1292/rc

© Quantitative Imaging in Medicine and Surgery. All rights reserved.

Conflicts of Interest: All authors have completed the ICMJE uniform disclosure form (available at https://qims.amegroups.com/article/view/10.21037/qims-23-1292/coif). The authors have no conflicts of interest to declare.

Ethical Statement: The authors are accountable for all aspects of the work in ensuring that questions related to the accuracy or integrity of any part of the work are appropriately investigated and resolved. The study was conducted in accordance with the Declaration of Helsinki (as revised in 2013). The study was approved by the Medical Ethics Committee of Tongji Hospital, Tongji Medical College, Huazhong University of Science and Technology (No. TJ-IRB20220413) and informed consent was taken from all individual participants.

Open Access Statement: This is an Open Access article distributed in accordance with the Creative Commons Attribution-NonCommercial-NoDerivs 4.0 International License (CC BY-NC-ND 4.0), which permits the non-commercial replication and distribution of the article with the strict proviso that no changes or edits are made and the original work is properly cited (including links to both the formal publication through the relevant DOI and the license). See: https://creativecommons.org/licenses/by-nc-nd/4.0/.

References

1. Quock TP, Yan T, Chang E, Guthrie S, Broder MS. Epidemiology of AL amyloidosis: a real-world study using US claims data. Blood Adv 2018;2:1046-53.
2. Dubrey SW, Cha K, Anderson J, Chamarthi B, Reisinger J, Skinner M, Falk RH. The clinical features of immunoglobulin light-chain (AL) amyloidosis with heart involvement. QJM 1998;91:141-57.
3. Kumar S, Dispenzieri A, Lacy MQ, Hayman SR, Buadi FK, Colby C, Laumann K, Zeldenrust SR, Leung N, Dingli D, Greipp PR, Lust JA, Russell SJ, Kyle RA, Rajkumar SV, Gertz MA. Revised prognostic staging system for light chain amyloidosis incorporating cardiac biomarkers and serum free light chain measurements. J Clin Oncol 2012;30:989-95.
4. Manwani R, Cohen O, Sharpley F, Mahmood S, Sachchithanantham S, Foard D, Lachmann HJ, Quarta C, Fontana M, Gillmore JD, Whelan C, Hawkins PN, Wechalekar AD. A prospective observational study of 915 patients with systemic AL amyloidosis treated with upfront bortezomib. Blood 2019;134:2271-80.
5. Dorbala S, Cuddy S, Falk RH. How to Image Cardiac Amyloidosis: A Practical Approach. JACC Cardiovasc Imaging 2020;13:1368-83.
6. Dorbala S, Ando Y, Bokhari S, Dispenzieri A, Falk RH, Ferrari VA, et al. Addendum to ASNC/AHA/ASE/EANM/HFSA/ISA/SCMR/SNMMI Expert Consensus Recommendations for Multimodality Imaging in Cardiac Amyloidosis: Part 1 of 2-Evidence Base and Standardized Methods of Imaging. J Card Fail 2022;28:e1-4.
7. Phelan D, Collier P, Thavendiranathan P, Popović ZB, Hanna M, Plana JC, Marwick TH, Thomas JD. Relative apical sparing of longitudinal strain using two-dimensional speckle-tracking echocardiography is both sensitive and specific for the diagnosis of cardiac amyloidosis. Heart 2012;98:1442-8.
8. Pagourelias ED, Mirea O, Duchenne J, Van Cleemput J, Delforge M, Bogaert J, Kuznetsova T, Voigt JU. Echo Parameters for Differential Diagnosis in Cardiac Amyloidosis: A Head-to-Head Comparison of Deformation and Nondeformation Parameters. Circ Cardiovasc Imaging 2017;10:e005588.
9. Nicol M, Baudet M, Brun S, Harel S, Royer B, Vignon M, Lairez O, Lavergne D, Jaccard A, Attias D, Macron L, Gayat E, Cohen-Solal A, Arnulf B, Logeart D. Diagnostic score of cardiac involvement in AL amyloidosis. Eur Heart J Cardiovasc Imaging 2020;21:542-8.
10. Williams LK, Forero JF, Popovic ZB, Phelan D, Delgado D, Rakowski H, Wintersperger BJ, Thavendiranathan P. Patterns of CMR measured longitudinal strain and its association with late gadolinium enhancement in patients with cardiac amyloidosis and its mimics. J Cardiovasc Magn Reson 2017;19:61.
11. Boldrini M, Cappelli F, Chacko L, Restrepo-Cordoba MA, Lopez-Sainz A, Giannoni A, et al. Multiparametric Echocardiography Scores for the Diagnosis of Cardiac Amyloidosis. JACC Cardiovasc Imaging 2020;13:909-20.
12. Kyrouac D, Schiffer W, Lennep B, Fergestrom N, Zhang KW, Gorcsan J 3rd, Lenihan DJ, Mitchell JD. Echocardiographic and clinical predictors of cardiac amyloidosis: limitations of apical sparing. ESC Heart Fail 2022;9:385-97.
13. Rausch K, Scalia GM, Sato K, Edwards N, Lam AK, Platts DG, Chan J. Left atrial strain imaging differentiates cardiac amyloidosis and hypertensive heart disease. Int J Cardiovasc Imaging 2021;37:81-90.
14. Uzan C, Lairez O, Raud-Raynier P, Garcia R, Degand B, Christiaens LP, Rehman MB. Right ventricular longitudinal strain: a tool for diagnosis and prognosis in

© Quantitative Imaging in Medicine and Surgery. All rights reserved.

light-chain amyloidosis. Amyloid 2018;25:18-25.
15. Aimo A, Fabiani I, Giannoni A, Mandoli GE, Pastore MC, Vergaro G, Spini V, Chubuchny V, Pasanisi EM, Petersen C, Poggianti E, Taddei C, Castiglione V, Latrofa S, Panichella G, Sciaccaluga C, Georgiopoulos G, Passino C, Cameli M, Emdin M. Multi-chamber speckle tracking imaging and diagnostic value of left atrial strain in cardiac amyloidosis. Eur Heart J Cardiovasc Imaging 2022;24:130-41.
16. Brand A, Frumkin D, Hübscher A, Dreger H, Stangl K, Baldenhofer G, Knebel F. Phasic left atrial strain analysis to discriminate cardiac amyloidosis in patients with unclear thick heart pathology. Eur Heart J Cardiovasc Imaging 2021;22:680-7.
17. Dorbala S, Ando Y, Bokhari S, Dispenzieri A, Falk RH, Ferrari VA, et al. ASNC/AHA/ASE/EANM/HFSA/ISA/SCMR/SNMMI Expert Consensus Recommendations for Multimodality Imaging in Cardiac Amyloidosis: Part 1 of 2-Evidence Base and Standardized Methods of Imaging. Circ Cardiovasc Imaging 2021;14:e000029.
18. Elliott PM, Anastasakis A, Borger MA, Borggrefe M, Cecchi F, et al. 2014 ESC Guidelines on diagnosis and management of hypertrophic cardiomyopathy: the Task Force for the Diagnosis and Management of Hypertrophic Cardiomyopathy of the European Society of Cardiology (ESC). Eur Heart J 2014;35:2733-79.
19. Whelton PK, Carey RM, Aronow WS, Casey DE Jr, Collins KJ, Dennison Himmelfarb C, et al. 2017 ACC/AHA/AAPA/ABC/ACPM/AGS/APhA/ASH/ASPC/NMA/PCNA Guideline for the Prevention, Detection, Evaluation, and Management of High Blood Pressure in Adults: A Report of the American College of Cardiology/American Heart Association Task Force on Clinical Practice Guidelines. J Am Coll Cardiol 2018;71:e127-248.
20. Ternacle J, Krapf L, Mohty D, Magne J, Nguyen A, Galat A, Gallet R, Teiger E, Côté N, Clavel MA, Tournoux F, Pibarot P, Damy T. Aortic Stenosis and Cardiac Amyloidosis: JACC Review Topic of the Week. J Am Coll Cardiol 2019;74:2638-51.
21. Dolgin M, Association NYH, Fox AC, Gorlin R, Levin RI, New York Heart Association. Criteria Committee. Nomenclature and criteria for diagnosis of diseases of the heart and great vessels. 9th ed. Boston, MA: Lippincott Williams and Wilkins; 1994.
22. Voigt JU, Pedrizzetti G, Lysyansky P, Marwick TH, Houle H, Baumann R, Pedri S, Ito Y, Abe Y, Metz S, Song JH, Hamilton J, Sengupta PP, Kolias TJ, d'Hooge J, Aurigemma GP, Thomas JD, Badano LP. Definitions for a common standard for 2D speckle tracking echocardiography: consensus document of the EACVI/ASE/Industry Task Force to standardize deformation imaging. Eur Heart J Cardiovasc Imaging 2015;16:1-11.
23. Badano LP, Kolias TJ, Muraru D, Abraham TP, Aurigemma G, Edvardsen T, D'Hooge J, Donal E, Fraser AG, Marwick T, Mertens L, Popescu BA, Sengupta PP, Lancellotti P, Thomas JD, Voigt JU; . Standardization of left atrial, right ventricular, and right atrial deformation imaging using two-dimensional speckle tracking echocardiography: a consensus document of the EACVI/ASE/Industry Task Force to standardize deformation imaging. Eur Heart J Cardiovasc Imaging 2018;19:591-600.
24. Löfbacka V, Axelsson J, Pilebro B, Suhr OB, Lindqvist P, Sundström T. Cardiac transthyretin amyloidosis (99m)Tc-DPD SPECT correlates with strain echocardiography and biomarkers. Eur J Nucl Med Mol Imaging 2021;48:1822-32.
25. Huntjens PR, Zhang KW, Soyama Y, Karmpalioti M, Lenihan DJ, Gorcsan J 3rd. Prognostic Utility of Echocardiographic Atrial and Ventricular Strain Imaging in Patients With Cardiac Amyloidosis. JACC Cardiovasc Imaging 2021;14:1508-19.
26. Ternacle J, Bodez D, Guellich A, Audureau E, Rappeneau S, Lim P, Radu C, Guendouz S, Couetil JP, Benhaiem N, Hittinger L, Dubois-Randé JL, Plante-Bordeneuve V, Mohty D, Deux JF, Damy T. Causes and Consequences of Longitudinal LV Dysfunction Assessed by 2D Strain Echocardiography in Cardiac Amyloidosis. JACC Cardiovasc Imaging 2016;9:126-38.
27. Licordari R, Minutoli F, Cappelli F, Micari A, Colarusso L, Di Paola FAF, Campisi M, Recupero A, Mazzeo A, Di Bella G. Mid-basal left ventricular longitudinal dysfunction as a prognostic marker in mutated transthyretin-related cardiac amyloidosis. Vessel Plus 2022;6:12.
28. Miglioranza MH, Badano LP, Mihăilă S, Peluso D, Cucchini U, Soriani N, Iliceto S, Muraru D. Physiologic Determinants of Left Atrial Longitudinal Strain: A Two-Dimensional Speckle-Tracking and Three-Dimensional Echocardiographic Study in Healthy Volunteers. J Am Soc Echocardiogr 2016;29:1023-1034.e3.
29. Sciacca V, Eckstein J, Körperich H, Fink T, Bergau L, El Hamriti M, Imnadze G, Guckel D, Fox H, Gerçek M, Farr M, Burchert W, Sommer P, Sohns C, Piran M. Magnetic-Resonance-Imaging-Based Left Atrial Strain and Left Atrial Strain Rate as Diagnostic Parameters in Cardiac Amyloidosis. J Clin Med 2022;11:3150.
30. Bodez D, Ternacle J, Guellich A, Galat A, Lim P, Radu

© Quantitative Imaging in Medicine and Surgery. All rights reserved.

C, Guendouz S, Bergoend E, Couetil JP, Hittinger L, Dubois-Randé JL, Plante-Bordeneuve V, Deux JF, Mohty D, Damy T. Prognostic value of right ventricular systolic function in cardiac amyloidosis. Amyloid 2016;23:158-67.
31. Moñivas Palomero V, Durante-Lopez A, Sanabria MT, Cubero JS, González-Mirelis J, Lopez-Ibor JV, Navarro Rico SM, Krsnik I, Dominguez F, Mingo AM, Hernandez-Perez FJ, Cavero G, Santos SM. Role of Right Ventricular Strain Measured by Two-Dimensional Echocardiography in the Diagnosis of Cardiac Amyloidosis. J Am Soc Echocardiogr 2019;32:845-853.e1.
32. Licordari R, Minutoli F, Recupero A, Campisi M, Donato R, Mazzeo A, Dattilo G, Baldari S, Vita G, Zito C, Di Bella G. Early Impairment of Right Ventricular Morphology and Function in Transthyretin-Related Cardiac Amyloidosis. J Cardiovasc Echogr 2021;31:17-22.
33. Di Bella G, Cappelli F, Licordari R, Piaggi P, Campisi M, Bellavia D, Minutoli F, Gentile L, Russo M, de Gregorio C, Perfetto F, Mazzeo A, Falletta C, Clemenza F, Vita G, Carerj S, Aquaro GD. Prevalence and diagnostic value of extra-left ventricle echocardiographic findings in transthyretin-related cardiac amyloidosis. Amyloid 2022;29:197-204.
34. Shi J, Wu Y, Wu B, Yu D, Chu Y, Yu F, Han D, Ye T, Tao X, Yang J, Wang X. Left ventricular myocardial work index and short-term prognosis in patients with light-chain cardiac amyloidosis: a retrospective cohort study. Quant Imaging Med Surg 2023;13:133-44.
35. Aimo A, Merlo M, Porcari A, Georgiopoulos G, Pagura L, Vergaro G, Sinagra G, Emdin M, Rapezzi C. Redefining the epidemiology of cardiac amyloidosis. A systematic review and meta-analysis of screening studies. Eur J Heart Fail 2022;24:2342-51.

Cite this article as: Huang PN, Liu YN, Cheng XQ, Liu HY, Zhang J, Li L, Sun J, Gao YP, Lu RR, Gao YP, Deng YB. Relative apical sparing obtained with speckle tracking echocardiography is not a sensitive parameter for diagnosing light-chain cardiac amyloidosis. Quant Imaging Med Surg 2024;14(3):2357-2369. doi: 10.21037/qims-23-1292

© Quantitative Imaging in Medicine and Surgery. All rights reserved.